THE JOURNAL OF BIOLOGICAL CHEMISTRY VOL. 281, NO. 3, pp. 1778–1783, January 20, 2006
© 2006 by The American Society for Biochemistry and Molecular Biology, Inc. Printed in the U.S.A.

The *Schizosaccharomyces pombe* Replication Inhibitor Spd1 Regulates Ribonucleotide Reductase Activity and dNTPs by Binding to the Large Cdc22 Subunit*

Received for publication, October 31, 2005, and in revised form, November 22, 2005 Published, JBC Papers in Press, November 28, 2005, DOI 10.1074/jbc.M511716200

Pelle Håkansson[1], **Lina Dahl, Olga Chilkova, Vladimir Domkin, and Lars Thelander**

From the Department of Medical Biochemistry and Biophysics, Umeå University, SE-901 87 Umeå, Sweden

Ribonucleotide reductase (RNR) is an essential enzyme that provides the cell with a balanced supply of deoxyribonucleoside triphosphates for DNA replication and repair. Mutations that affect the regulation of RNR in yeast and mammalian cells can lead to genetic abnormalities and cell death. We have expressed and purified the components of the RNR system in fission yeast, the large subunit Cdc22p, the small subunit Suc22p, and the replication inhibitor Spd1p. It was proposed (Liu, C., Powell, K. A., Mundt, K., Wu, L., Carr, A. M., and Caspari, T. (2003) *Genes Dev.* 17, 1130–1140) that Spd1 is an RNR inhibitor, acting by anchoring the Suc22p inside the nucleus during G_1 phase. Using *in vitro* assays with highly purified proteins we have demonstrated that Spd1 indeed is a very efficient inhibitor of fission yeast RNR, but acting on Cdc22p. Furthermore, biosensor technique showed that Spd1p binds to the Cdc22p with a K_D of 2.4 μM, whereas the affinity to Suc22p is negligible. Therefore, Spd1p inhibits fission yeast RNR activity by interacting with the Cdc22p. Similar to the situation in budding yeast, logarithmically growing fission yeast increases the dNTP pools 2-fold after 3 h of incubation in the UV mimetic 4-nitroquinoline-*N*-oxide. This increase is smaller than the increase observed in budding yeast but of the same order as the dNTP pool increase when synchronous *Schizosaccharomyces pombe cdc10* cells are going from G_1 to S-phase.

Looking for novel fission yeast genes that cause cell cycle arrest when overexpressed, Woollard *et al.* (1) cloned *spd1* (for S-phase delayed). The encoded 14-kDa protein is cell cycle-regulated, and the levels decline during S-phase. Overexpression of *spd1* inhibits G_1/S progression downstream of Start, but it is not an essential gene. In a later publication, Borgne and Nurse (2) demonstrated that overexpression of Spd1p blocks the onset of both S-phase and mitosis, and they suggested that the protein might act by interfering directly with DNA replication giving the same phenotype as that seen using the ribonucleotide reductase (RNR)[2] inhibitor hydroxyurea.

Null mutants of the fission yeast *csn1-d* and *csn2-d* signalosome subunits are slow growing and have a prolonged S-phase (3). In a screen for multicopy suppressors of *rad3-ts csn1-d* lethality to identify the cause of the slow S-phase in signalosome mutants, Liu *et al.* (4) identified multiple independent clones of *suc22* that rescued the growth defect. *Suc22* encodes the small subunit of *Schizosaccharomyces pombe* RNR that together with the large subunit Cdc22p forms the active enzyme complex (5). Because the phenotype of *spd1* overexpression resembled the phenotype of *csn1-d or csn2-d* mutants, Liu *et al.* combined the deletion of *spd1* with either of the signalosome subunit mutants, and in both cases, loss of *spd1* restored the normal cell cycle profile. They concluded from these experiments that Spd1p inhibits RNR activity and that the signalosome complex is required to release the inhibition during DNA replication or repair.

Using indirect immunofluorescence microscopy, Liu *et al.* observed nuclear co-localization of Suc22p and Spd1p. Although no direct evidence was presented for interaction between the proteins, such an interaction was assumed in a model for the regulation of fission yeast RNR activity during S-phase and DNA repair. According to this model, Spd1p anchors the Suc22p inside the nucleus, thereby inhibiting RNR activity. To increase the supply of deoxyribonucleotides during DNA replication or repair, Spd1p is destroyed by the signalosome; this leads to a delocalization of the Suc22p from the nucleus to the cytoplasm where it combines with the Cdc22p to form active RNR. This model is cited in a number of publications and reviews (6–9).

In this report, we describe the expression and purification of the Cdc22p, Suc22p, and Spd1p and demonstrate by *in vitro* assays with highly purified recombinant proteins that Spd1p is a strong inhibitor of fission yeast RNR acting on Cdc22p. Furthermore, biosensor technique using chips with immobilized Spd1p shows that the inhibitor specifically binds to Cdc22p with a dissociation constant of 2.4 μM, whereas the affinity to Suc22p is negligible. Our data support a model where Spd1 regulates RNR activity by binding to the Cdc22p and not to the Suc22p. This mode of regulation is similar to the regulation of RNR activity in budding yeast, where binding of the low molecular weight inhibitor Sml1 to the Cdc22p homologue, the Rnr1p, controls RNR activity.

Logarithmically growing budding yeast dramatically improves survival following DNA damage by increasing the deoxyribonucleotide pools to values much higher than in S-phase cells (10). We also observe an increase in deoxyribonucleotide pools in fission yeast after DNA damage. However, the increase is only 2-fold and of the same order as the increase in dNTP pools in synchronized, undamaged S-phase cells compared with G_1 cells.

EXPERIMENTAL PROCEDURES

Growth of Fission Yeast—Wt and the ts mutant strain *cdc10-V50* were grown in YE medium. Synchronization of the *cdc10* strain was accomplished by first growing the cells at 25 °C, shifting to 36 °C for 4 h, and then shifting back again to 25 °C (1). Flow cytometry was made according to Ref. 11 using a Beckman Cytomics FC 500 machine.

Protein Expression and Purification—Cdc22p, Suc22p, and Spd1p were expressed in *Escherichia coli* BL21(DE3)pLysS bacteria using the

* This work was supported by the Swedish Research Council, the Medical Faculty of Umeå University, the Kempe Foundation, and by a fellowship from the Royal Swedish Academy of Sciences (to V. D.). The costs of publication of this article were defrayed in part by the payment of page charges. This article must therefore be hereby marked "*advertisement*" in accordance with 18 U.S.C. Section 1734 solely to indicate this fact.

[1] To whom correspondence should be addressed. Tel.: 46-907865263; Fax: 46-907869795; E-mail: pelle.hakanson@medchem.umu.se.

[2] The abbreviations used are: RNR, ribonucleotide reductase; wt, wild type; RU, resonance unit; HPLC, high pressure liquid chromatography; EPR, electron paramagnetic resonance; 4-NQO, 4-nitroquinoline-*N*-oxide.

This is an Open Access article under the CC BY license.

pET3a expression vector (Novagen). Plasmids containing the *cdc22* and *suc22* genes, pCDC22–1 and pSUC22–1, were gifts from Christopher J. McInerny, University of Glasgow, UK. A cDNA clone of *spd1* (ARC 640:Spd1cDNA) in pREP41X was obtained from Paul Nurse. To remove the intron in *cdc22*, the AatII site in pET 3a was first destroyed by cutting, removing the protruding 3′-tail with T4 DNA polymerase, and religation. A synthetic linker encoding the first 9 amino acid residues in Cdc22p including an AatII site followed by an NsiI restriction site was cloned into the pET3a opened with NdeI and BamH1. A fragment lacking the intron but containing the major part of the Cdc22p coding sequence was prepared by digesting the pCDC22–1 with AatII and NsiI (cutting downstream of the stop codon) and ligating into the pET vector opened with the same restriction enzymes.

The Cdc22p was expressed by growing the bacterial culture in TB medium plus 100 μg/ml of carbenicillin and 34 μg/ml of chloramphenicol at 30 °C to $A_{600} = 2$. Then the incubator was set at 15 °C, isopropyl 1-thio-β-D-galactopyranoside was added to a final concentration of 0.2 mM, and the culture was allowed to grow at 15 °C overnight. Cdc22p was purified by ammonium sulfate fractionation and affinity chromatography on dATP-Sepharose as described (12).

Suc22p-expressing bacteria were grown in Luria Bertani medium containing the same antibiotics as above at 30 °C to an $A_{600} = 0.7$ when isopropyl 1-thio-β-D-galactopyranoside was added to a final concentration of 0.4 mM and the culture incubated for another 3 h at 30 °C. Suc22p was purified by streptomycin sulfate precipitation, ammonium sulfate precipitation to 50% saturation (0.295 g/ml), and chromatography on DEAE-Sepharose fast flow essentially as described earlier (13). Instead of stepwise elution, the protein was eluted by a linear gradient of 0–500 mM NaCl in 10 mM potassium phosphate buffer, pH 7.0, where Suc22p eluted around 250 mM NaCl. The final Suc22p preparations contained 0.2–0.4 mol tyrosyl radical/mol of polypeptide chain.

The Spd1p-expressing bacteria were grown the same way as the Suc22p-expressing bacteria but at 37 °C, and they were induced with isopropyl 1-thio-β-D-galactopyranoside at a final concentration of 0.5 mM. After lysing the bacteria by freezing and thawing, the crude extract was centrifuged for 60 min at 45,000 rpm at 4 °C in a Beckman Ti-70 rotor, and the supernatant was discarded. The pellet was washed three times with 50 mM Tris-Cl, pH 7.4, treated with DNase 1 (5 μg/ml), and dissolved in 0.1 M Tris-Cl, pH 8.5, 5 M urea. After incubation for 20 min on ice, the solution was centrifuged at 45,000 × *g* for 20 min at 4 °C and the pellet discarded. Finally, the urea-solubilized Spd1p was refolded by instant 10× dilution in 50 mM Tris-Cl, pH 7.5, 100 mM potassium acetate; the remaining urea was removed by gel filtration on a Sephadex G50 column equilibrated with the same buffer.

RNR Assay—Assay mixtures containing 20 mM Hepes-KOH (pH 7.3), 100 mM KOAc, 5 mM ATP, 20 mM $Mg(OAc)_2$, 0.5 mM [^{3}H]cytidine 5′-diphosphate (CDP; specific activity 22400 cpm/nmol), 20 μM $FeCl_3$, 20 mM dithiothreitol, and RNR proteins in different combinations were incubated at 25 °C for 25 min in a final volume of 50 μl. After incubation, the samples were processed as described earlier to obtain the amount of dCDP formed (14). Molar concentrations of Cdc22p, Suc22p, and Spd1p are calculated using the monomer molecular weights of 92,000, 45,400, and 14,200, respectively.

BIAcore Biosensor Analysis—The interaction between Spd1p and Cdc22p, Suc22p, budding yeast Rnr1p, Sml1p, and mouse R1 protein was studied by biosensor analysis using a BIAcore 2000 (Biacore International AB). The Spd1p was prepared in 50 mM potassium phosphate buffer, pH 7.0, at a concentration of 0.07 mg/ml; it was then immobilized on a CM5 sensor chip (BIAcore) as described earlier (15). Immobilization of the budding yeast Sml1p was made as in Ref. 16. All ligand proteins were equilibrated with running buffer (10 mM Hepes-KOH, pH 7.4, 200 mM KOAc, 1 mM EDTA, 5 mM MgOAc, and 0.005% Surfactant P 20 (BIAcore). The interactions were studied at a constant temperature of 20 °C and a constant flow of 70 μl/min. Kinetics for the interaction of Spd1p with Cdc22p was determined by allowing the immobilized Spd1p to interact with increasing concentrations of Cdc22p (17). Between each injection, bound protein was removed by washing with 5 μl of 5 mM NaOH. The resonance unit (RU) is proportional to the mass, and 1 RU corresponds to a surface concentration of 1 pg of protein/mm^2 of the CM5 sensor chip (18).

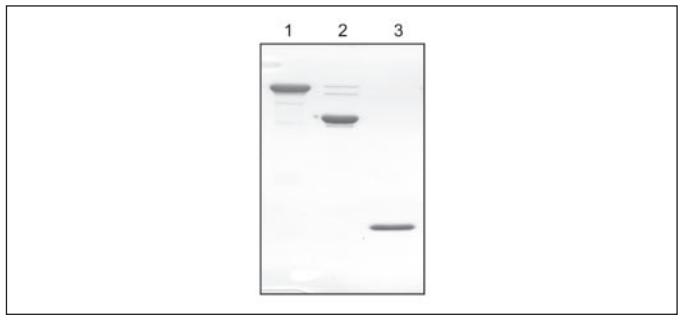

FIGURE 1. **SDS-polyacrylamide gel electrophoresis analysis of 2 μg each of recombinant *S. pombe* Cdc22p (*lane 1*), Suc22p (*lane 2*), and Spd1p (*lane 3*).** The 12% polyacrylamide gel was stained by Coomassie Brilliant Blue.

Determination of NTP and dNTP Pools by HPLC—Cells were harvested by filtration through 25-mm White AAWP nitrocellulose filters (0.8 μm; Millipore) that were immediately immersed in ice-cold extraction solution (10% w/v trichloroacetic acid, 15 mM $MgCl_2$) (10). Separation and quantitation of dNTPs and NTPs using HPLC were carried out as described in Ref. 19 with the following modification. To improve the sensitivity, we used a Poly WAX LP, 200 × 4.6 mm, 5-μm, 300-E column (PolyLC Inc.) instead of the Partisphere SAX-5 column. The column was run isocratically in 0.29 M potassium phosphate buffer, pH 5.0, 2% (v/v) acetonitrile at 1.0 ml/min.

RESULTS

Expression and Purification of Recombinant S. pombe Cdc22p, Suc22p, and Spd1p—The results from an SDS-polyacrylamide gel electrophoresis analysis of our highly purified recombinant *S. pombe* proteins are shown in Fig. 1. Unexpectedly, the 124-amino acid residue Spd1p formed almost exclusively inclusion bodies when expressed at 37 °C. Initially, we therefore grew the bacteria at 20 °C for 3 h after isopropyl 1-thio-β-D-galactopyranoside induction, which resulted in soluble protein. However, the yield was much better and the purity of the final preparation higher when we expressed Spd1p as inclusion bodies followed by solubilization in urea and rapid dilution into urea-free buffer (Fig. 1). The soluble and the solubilized forms of Spd1p both showed the same capacity to inhibit the *S. pombe* RNR system *in vitro* (data not shown). The lack of cysteine residues in Spd1p may explain the stability of the protein.

Properties of the S. pombe RNR System—Electron paramagnetic resonance analysis of the highly purified Suc22p showed that it contained a tyrosyl free radical giving a signal similar to the EPR signal of the mouse RNR R2 protein or the Rnr2p of *Saccharomyces cerevisiae* (data not shown). The specific activity of Cdc22p assayed at 25 °C in the presence of an excess of Suc22p was ~10 nmol dCDP/mg of protein/min, and the specific activity of Suc22p assayed at 25 °C in the presence of an excess of Cdc22p was ~400 nmol dCDP/mg of protein/min. These specific activities are closer to the values of the mouse RNR R1 and R2 proteins, 130 and 280, respectively, assayed at 37 °C (12, 20) than the values of the

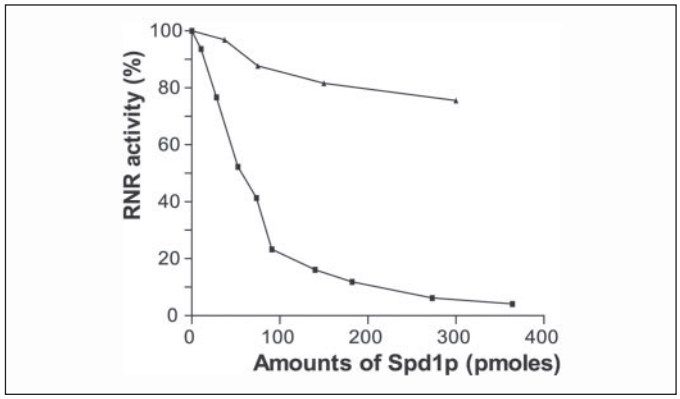

FIGURE 2. **Inhibition of RNR by Spd1p.** A series of tubes containing fission yeast RNR (100 pmol Cdc22p and 550 pmol Suc22p) were incubated under standard assay conditions for 25 min (■-■). In addition, the tubes contained increasing amounts of Spd1p. 100% activity corresponds to the formation of 1.9 nmol dCDP. The assay was also made with a heterologous system consisting of budding yeast Rnr1p (100 pmol) and fission yeast Suc22p (550 pmol) (▲-▲). In this combination, 100% activity corresponds to the formation of 4.9 nmol dCDP.

budding yeast Rnr1p and Rnr2p/Rnr4p, 250 and 2250, respectively, assayed at 30 °C (21, 22). Like other class 1 RNRs, the *S. pombe* enzyme is feedback inhibited by dATP with a 50% inhibition of the 5-mM ATP-stimulated reaction at 40 μM dATP.

Inhibition by Spd1p—Recombinant Cdc22p plus Suc22p was assayed for activity using the CDP reduction assay, with ATP as a positive effector in the presence of increasing amounts of Spd1 protein (Fig. 2). Under these conditions 50% inhibition was already observed at 1 μM concentration of Spd1p. The inhibition was highly specific for *S. pombe* RNR because very little inhibition was observed when Spd1p was added to an assay system containing Rnr1p plus Rnr2p/Rnr4p of *S. cerevisiae* or an assay system containing mouse R1 plus R2 proteins (data not shown).

To differentiate between inhibition of Suc22p and Cdc22p activity by Spd1p, we took advantage of the observation that budding yeast Rnr1p forms an active RNR complex with fission yeast Suc22p, although the amino acid sequence identity is only 66% between Rnr1p and Cdc22p. Assaying recombinant budding yeast Rnr1p plus Suc22p for activity using the CDP reduction assay in the presence of increasing amounts of Spd1 protein showed very little inhibition compared with the results with Cdc22p and Suc22p (Fig. 2). Because Spd1 is a very weak inhibitor of the budding yeast RNR, these results strongly indicate that Spd1 inhibits the fission yeast RNR by specifically interacting with Cdc22p.

To find out more about the inhibition mechanism, we prepared a series of assay tubes containing a fixed amount of Cdc22p (85 pmol) and increasing amounts of Suc22p with and without a constant amount of Spd1p (90 pmol) (Fig. 3*A*). In the absence of added Spd1p, the activity increased with increasing amounts of Suc22p up to 330 pmol, when a plateau was reached. Addition of Spd1 resulted in an almost constant inhibition in all tubes of ~80%. We then prepared another series of assay tubes containing a fixed amount of Suc22p (10 pmol) and increasing amounts of Cdc22p with and without a constant amount of Spd1 (50 pmol) (Fig. 3*B*). The activity increased with increasing amounts of Cdc22p in the absence of Spd1 to reach a plateau at ~300 pmol protein. In the presence of Spd1p, there was an initial inhibition of ~50%, but this inhibition decreased to 10% on the addition of increasing amounts of Cdc22p. These results again supported that Spd1p mainly inhibits the Cdc22p activity and not the Suc22p activity.

Kinetic Studies of the Interaction between the Cdc22p, Suc22p, and Spd1p Using a Biosensor Technique—To determine whether Spd1p interacts with Cdc22p, Suc22p, or both, we immobilized the Spd1 protein to a dextran layer on a sensor chip and then injected a series of

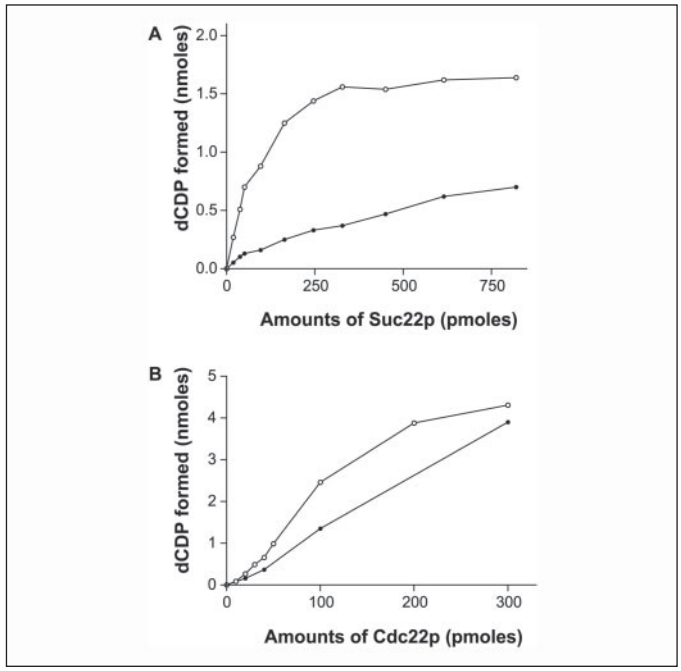

FIGURE 3. **Spd1p mainly interferes with Cdc22p activity.** *A*, titration of Cdc22p by Suc22p in the absence and in the presence of Spd1p. A series of tubes containing 85 pmol Cdc22p with (●-●) or without (○-○) 90 pmol Spd1p were assayed under standard conditions in the presence of increasing amounts of Suc22p. *B*, titration of Suc22p by Cdc22p in the absence and in the presence of Spd1p. A series of tubes containing 10 pmol Suc22p with (●-●) or without (○-○) 50 pmol Spd1p were assayed in the presence of increasing amounts of Cdc22p.

solutions containing increasing concentrations of Cdc22p or Suc22p to the same sensor chip. The immobilization of Spd1p at a concentration of 0.07 mg/ml gave an increase of 200 RU, which corresponds to 200 pg/mm^2. With a surface of 0.8 mm^2, 200 RU corresponds to a total of 160 pg of bound Spd1p, which can be compared with the total injected amount of 210 ng. This low degree of attachment (only 0.08%) makes it unlikely that the Spd1p is attached to multiple binding sites.

Injection of increasing concentrations of Cdc22p resulted in increasing equilibrium values (Fig. 4*A*). A Scatchard plot of the response at equilibrium of increasing concentrations of Cdc22p interacting with a constant amount of immobilized Spd1p gave an equilibrium dissociation constant K_D of 2.4 μM and a maximal binding of 0.43 mol Cdc22p monomer/mol of immobilized Spd1p (data not shown). Injection of Suc22p resulted in very low binding; low binding was also observed after the injection of *S. cerevisiae* Rnr1p or mouse R1 protein (Fig. 4*A*). Injection of an equimolar solution of Cdc22p and Suc22p resulted in a small but reproducible decrease in equilibrium value compared with the injection of Cdc22p alone. Addition of 0.1 mM dTTP to the injection mixture, known to induce dimerization of the large subunit of mouse and budding yeast RNR (16), had no major effect on the sensorgram. As a comparison we immobilized *S. cerevisiae* Sml1p to a sensor chip (Fig. 4*B*). Injection of *S. cerevisiae* Rnr1p resulted in an efficient binding, whereas injection of Cdc22p or Suc22p gave no significant binding.

Changes in Deoxyribonucleoside Triphosphate Pools in Fission Yeast after DNA Damage and during the Cell Cycle—Budding yeast regulates RNR activity during DNA replication and repair by binding of the low molecular weight protein inhibitor Sml1p to Rnr1p (16, 23). When budding yeast enters S-phase or after DNA damage, Sml1p is degraded, releasing RNR from inhibition and resulting in elevated dNTP pools (10, 23, 24). It was reported that Ddb1/Csn1/Csn2/Cullin 4-mediated degradation of Spd1p is essential for DNA replication and repair in fission

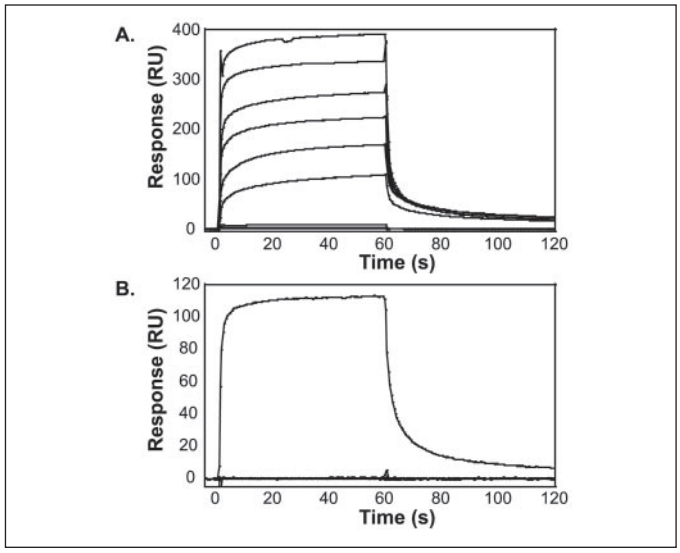

FIGURE 4. *A*, sensorgram showing the interaction between immobilized Spd1p (200 RU) and increasing concentrations of mobile phase Cdc22p (from the top 32, 16, 8, 4, 2, and 1 μM), *S. cerevisiae* Rnr1 (2 μM; *second from the baseline*), or Suc22p (2 μM; *first from the baseline*). Mouse R1 protein at 2 μM gave approximately the same curve as Rnr1p (data not shown). Injection starts at 0 s and ends at 60 s. The bulk effect responses of buffer components and the contribution from immobilized Spd1p have been subtracted. *B*, sensorgram showing the interaction between immobilized *S. cerevisiae* Sml1p (240 RU) and mobile phase *S. cerevisiae* Rnr1p, Cdc22p, or Suc22p, all at a concentration of 2 μM. The curves with Cdc22p and Suc22p cannot be clearly distinguished from the baseline.

yeast and that deletion of Ddb1 led to decreased dNTP pools in undamaged cells (4, 8).

Because Spd1p similar to Sml1p specifically inhibits RNR, we were interested to study whether and to what extent DNA damage affected the dNTP pools in logarithmically growing fission yeast. Like budding yeast (10), an increase in dNTP pools was already observed 1 h after the addition of 1 mg/liter of 4-nitroquinoline-*N*-oxide (4-NQO), a mutagen that acts as a UV mimetic (25), and after 3 h all four dNTP pools showed a 2-fold increase (Fig. 5*B*). Separate experiments using 0.2mg/liter of 4-NQO indicated that maximal pool increase was obtained at 1 mg/liter (data not shown). Flow cytometry of the culture before and 3 h after the addition of 4-NQO showed a small increase in G_1 cells and a small decrease in the number of S-phase cells after drug addition (Fig. 5*A*).

To be able to relate this DNA damage-induced dNTP pool increase to the dNTP levels in fission yeast during the cell cycle, we measured the pools in temperature-sensitive *cdc10* mutant cells shifted to 25 °C after 4 h of synchronization at 36 °C. Cells were harvested for flow cytometry and dNTP pool determinations 0, 45, 60, 75, and 90 min after the downshift in incubation temperature. A 2-fold increase in all dNTP pools was observed when the 0-min sample was compared with the 90-min sample (Fig. 5*D*). Flow cytometry showed that the cells were blocked in G_1 after 4 h at the restrictive temperature, proceeded into S-phase after 45 min at 25 °C, and after 90 min the majority of the cells had a DNA content >1C indicative of being in or just after S-phase (Fig. 5*C*). The dNTP pool increase observed in logarithmically growing wt cells after the addition of 4-NQO (Fig. 5*B*) was similar to the increase observed in 4-NQO-treated logarithmically growing *cdc10* cells.

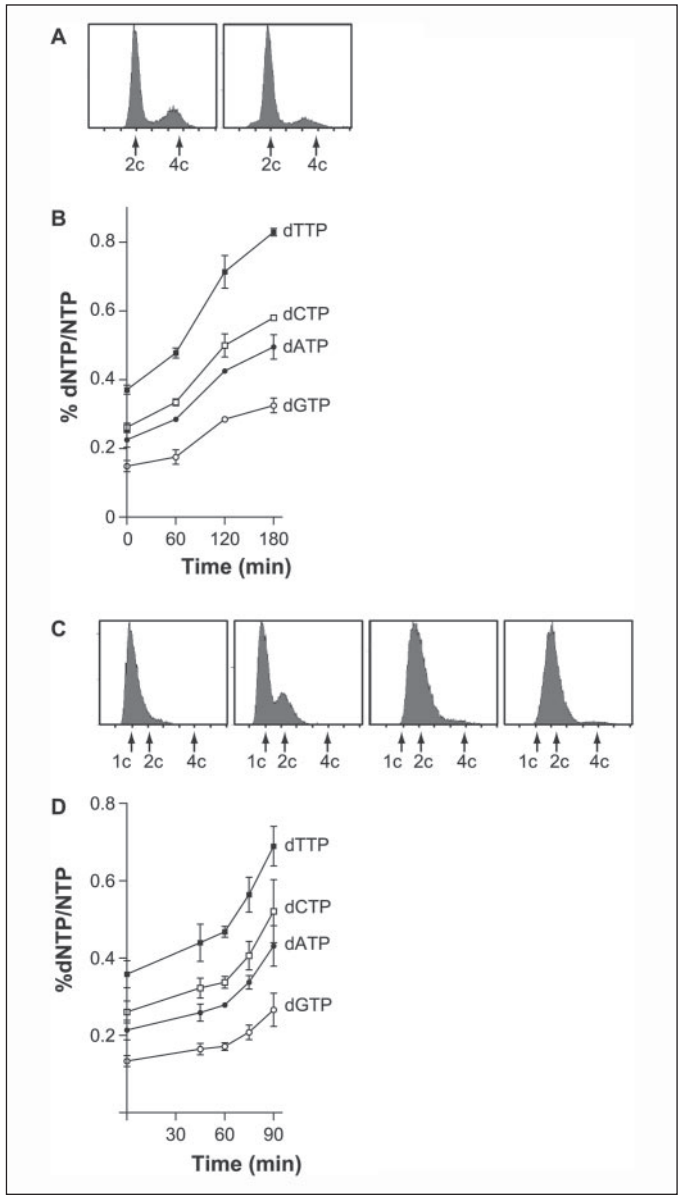

FIGURE 5. **Changes in dNTP levels in logarithmically growing fission yeast cells in response to DNA damage and in synchronized *cdc10* cells during the cell cycle.** To be able to compare wt to *cdc10* cells, all cells were grown at 25 °C. However, the dNTP pools in wt cells grown at 30 °C are not significantly different from the pools in cells grown at 25 °C (data not shown). *A*, flow cytometry of logarithmically growing wt cells without 4-NQO (*left*) and 3 h after the addition of 1 mg/l of 4-NQO (*right*). *B*, time-dependent changes in dNTPs after DNA damage. The *ordinate* gives each dNTP pool as % of the total ribonucleoside triphosphate pools (CTP+UTP+ATP+GTP). Because of the large variations in size in fission yeast cells, we find this way of presenting the data more meaningful than calculating the amounts of dNTP/cell (19). However, for comparison the dNTP levels in pmol/10^6 cells in logarithmically growing wt cells are 1.25, 0.95, 0.69, and 0.45 for dTTP, dCTP, dATP, and dGTP, respectively. The *abscissa* gives time in minutes after the addition of 4-NQO. *Error bars* represent S.D. of at least two independent measurements. *C*, flow cytometry of *cdc10* cells 0, 45, 75, and 90 min (*left to right*) after the shift to 25 °C after 4 h at 36 °C. *D*, time-dependent changes in dNTPs during the cell cycle with same ordinate as in *panel B*. *Error bars* represent S.D. of at least two independent measurements.

DISCUSSION

We have demonstrated in *in vitro* assays using highly purified proteins that Spd1p is an efficient inhibitor of fission yeast ribonucleotide reductase. However, in strong contrast to the model proposed by Liu *et al.* (4), biosensor technique showed that Spd1p has no affinity for the Suc22p but instead binds the Cdc22p with a K_D of 2.4 μM. The binding data are in full agreement with data from inhibition assays with the homologous Cdc22p/Suc22p system and the heterologous Rnr1p/Suc22p system where significant inhibition was only observed in the system containing Cdc22p. Therefore, it is highly unlikely that Spd1p acts by anchoring Suc22p inside the nucleus during the G_1 phase of the cell cycle as was proposed. Instead, our results are in agreement with the demonstration by Borgne and Nurse (2) that Spd1p is mainly localized

in the cytoplasm where it can directly control RNR activity by binding to the Cdc22p.

Liu *et al.* (4) observed that loss of *spd1* phenocopied *suc22* overexpression in *csn1-d* cells and interpreted their data to mean that Spd1p directly acted on Suc22p. However, as clearly seen in Fig. 3, the low affinity between the two subunits of fission yeast RNR, Cdc22p and Suc22p, similar to most type I RNRs, results in increased enzyme activity independent of which subunit is overexpressed when one subunit is present in low amounts.

Our results emphasize the similarities between the RNR systems in fission and budding yeast in that both regulate RNR activity during DNA replication and repair by a low molecular weight protein inhibitor, Spd1p and Sml1p, respectively (4, 16, 23). There is no sequence homology between the two inhibitors, and in the case of Sml1p, deletion of amino acid residues 2–50 from the total 104 amino acid residues had very little effect on the inhibition efficiency (26). In contrast, deletion of the first 29 amino acid residues from the total 124 amino acid residues in Spd1p resulted in a protein much less effective in causing cell cycle arrest when overexpressed than the intact protein (1). Sml1p is a target of the Mec1/Rad 53 kinase cascade, and its degradation after DNA damage is initiated by phosphorylation by the Dun1 kinase at serine 56, serine 58, and serine 60 (24, 27). In fission yeast, Ddb1, Cullin4, and the signalosome subunits Csn1 and Csn2 are required for the degradation of Spd1p (4, 8, 9), but up to now, no phosphorylation of Spd1p has been demonstrated. Inability to degrade Sml1p during S-phase or after DNA damage in budding yeast results in decreased dNTP levels, incomplete DNA replication, defective mitochondrial DNA propagation, and cell death (24). Likewise, the inability to degrade Spd1p in fission yeast results in decreased dNTP levels, increased mutation rate, slow S-phase progression, and inability to enter meiosis because of blocked premeiotic S-phase (1, 4, 8). The exact mechanism by which Spd1/Sml1 inhibits RNR activity is still unknown, but our results from *in vitro* assays indicate that there is no simple competition between Spd1/Sml1 and the small RNR subunit for binding to the large subunit (16).

In both budding and fission yeast, regulation of export of the small subunit from the nucleus to the cytoplasmatically localized large subunit was suggested to regulate RNR activity during S-phase and after DNA damage (4, 28). In mammalian cells, both RNR subunits were demonstrated to be localized to the cytoplasm during the cell cycle (29, 30). In contrast, the p53-inducible small subunit homologue, p53R2, was translocated from the cytoplasm to the nucleus after DNA damage (31). Our present results do not exclude transport of the small RNR subunit from the nucleus to the cytoplasm as a mechanism to regulate RNR activity in yeast cells.

In budding yeast, DNA damage was shown to increase the dNTP pools 6–8-fold, which resulted in dNTP levels 3–5-fold higher than the dNTP pools in untreated synchronized S-phase cells (10). This increase is possible because of a relaxed dATP feedback inhibition of budding yeast RNR. Even further increased pools strongly improved survival following DNA damage, but they also led to higher mutation rates. The fission yeast RNR shows a 50% feedback inhibition at 40 μM dATP compared with 10 and 80 μM for the mouse and budding yeast enzyme, respectively, all assayed in the presence of 5 mM ATP (10, 21). This relatively tight dATP feedback inhibition of the fission yeast RNR may be one explanation why the dNTP pools in logarithmically growing fission yeast only increased ~2-fold after DNA damage. Also, the fluctuations during the cell cycle are much less pronounced in fission yeast than in budding yeast, an ~2-fold increase for all dNTPs in fission yeast compared with a 6-fold increase in the purine dNTPs and a 3-fold increase in the pyrimidine dNTPs during S-phase in budding yeast (10, 32).

How does the regulation of RNR activity in fission and budding yeast compare with the regulation in mammalian cells? Common for all three organisms is that a failure to provide sufficient and balanced dNTP pools can lead to misincorporation of dNTPs into DNA, resulting in genetic abnormalities and cell death. So far, no low molecular weight protein inhibitor of the mammalian RNR has been identified, but the small size and the very low amino acid sequence conservation between Spd1p and Sml1p make it difficult to identify such an inhibitor in mammalian genome sequences. There are conflicting results in the literature regarding the effects of DNA damage on dNTP pools in mammalian cells (33). However, recent data from our laboratory show that mammalian cells do not increase their dNTP pools after DNA damage and still the dNTP pools in G_1 cells are only 1/20 of the pools in S-phase cells,[3] indicating a regulation different from the regulation in yeast.

Acknowledgments—We thank Christopher J. McInerny and Paul Nurse for providing plasmids, Karl Ekwall for providing fission yeast strains, Erik Boye for help with flow cytometry, and Nina Voevodskaya for performing the EPR analysis.

REFERENCES

1. Woollard, A., Basi, G., and Nurse, P. (1996) *EMBO J.* **15,** 4603–4612
2. Borgne, A., and Nurse, P. (2000) *J. Cell Sci.* **113,** 4341–4350
3. Mundt, K. E., Porte, J., Murray, J. M., Brikos, C., Christensen, P. U., Caspari, T., Hagan, I. M., Millar, J. B., Simanis, V., Hofmann, K., and Carr, A. M. (1999) *Curr. Biol.* **9,** 1427–1430
4. Liu, C., Powell, K. A., Mundt, K., Wu, L., Carr, A. M., and Caspari, T. (2003) *Genes Dev.* **17,** 1130–1140
5. Fernandez-Sarabia, M. J., McInerny, C., Harris, P., Gordon, C., and Fantes, P. (1993) *Mol. Gen. Genet.* **238,** 241–251
6. Nielsen, O. (2003) *Curr. Biol.* **13,** R565-R567
7. Bondar, T., Ponomarev, A., and Raychaudhuri, P. (2004) *J. Biol. Chem.* **279,** 9937–9943
8. Holmberg, C., Fleck, O., Hansen, H. A., Liu, C., Slaaby, R., Carr, A. M., and Nielsen, O. (2005) *Genes Dev.* **19,** 853–862
9. Liu, C., Poitelea, M., Watson, A., Yoshida, S., Shimoda, C., Holmberg, C., Nielsen, O., and Carr, A. M. (2005) *EMBO J.*, in press
10. Chabes, A., Georgieva, B., Domkin, V., Zhao, X., Rothstein, R., and Thelander, L. (2003) *Cell* **112,** 391–401
11. Nilssen, E. A., Synnes, M., Kleckner, N., Grallert, B., and Boye, E. (2003) *Proc. Natl. Acad. Sci. U. S. A.* **100,** 10758–10763
12. Davis, R., Thelander, M., Mann, G. J., Behravan, G., Soucy, F., Beaulieu, P., Lavallée, P., Gräslund, A., and Thelander, L. (1994) *J. Biol. Chem.* **269,** 23171–23176
13. Rova, U., Adrait, A., Pötsch, S., Gräslund, A., and Thelander, L. (1999) *J. Biol. Chem.* **274,** 23746–23751
14. Engström, Y., Eriksson, S., Thelander, L., and Åkerman, M. (1979) *Biochemistry* **18,** 2941–2948
15. Rova, U., Goodtzova, K., Ingemarson, R., Behravan, G., Gräslund, A., and Thelander, L. (1995) *Biochemistry* **34,** 4267–4275
16. Chabes, A., Domkin, V., and Thelander, L. (1999) *J. Biol. Chem.* **274,** 36679–36683
17. Ingemarson, R., and Thelander, L. (1996) *Biochemistry* **35,** 8603–8609
18. Jönsson, U., Fägerstam, L., Ivarsson, B., Johnsson, B., Karlsson, R., Lundh, K., Löfås, S., Persson, B., Roos, H., Rönnberg, I., Sjölander, S., Stenberg, E., Ståhlberg, R., Urbaniczky, C., Östlin, H., and Malmqvist, M. (1991) *BioTechniques* **11,** 620–627
19. Hofer, A., Ekanem, J. T., and Thelander, L. (1998) *J. Biol. Chem.* **273,** 34098–34104
20. Mann, G. J., Gräslund, A., Ochiai, E.-I., Ingemarson, R., and Thelander, L. (1991) *Biochemistry* **30,** 1939–1947
21. Domkin, V., Thelander, L., and Chabes, A. (2002) *J. Biol. Chem.* **277,** 18574–18578
22. Chabes, A., Domkin, V., Larsson, G., Liu, A., Gräslund, A., Wijmenga, S., and Thelander, L. (2000) *Proc. Natl. Acad. Sci. U. S. A.* **97,** 2474–2479
23. Zhao, X., Muller, E. G., and Rothstein, R. (1998) *Mol. Cell* **2,** 329–340
24. Zhao, X., Chabes, A., Domkin, V., Thelander, L., and Rothstein, R. (2001) *EMBO J.* **20,** 3544–3553
25. Friedberg, E. C., Walker, G. C., and Siede, W. (1995) *DNA Repair and Mutagenesis*, p. 42, American Society for Microbiology, Washington, D.C.

[3] P. Håkansson, A. Hofer, and L. Thelander, manuscript in preparation.

26. Zhao, X., Georgieva, B., Chabes, A., Domkin, V., Ippel, J., Schleucher, J., Wijmenga, S., Thelander, L., and Rothstein, R. (2000) *Mol. Cell. Biol.* **20,** 9076–9083
27. Uchiki, T., Dice, L. T., Hettich, R. L., and Dealwis, C. (2003) *J. Biol. Chem.* **279,** 11293–11303
28. Yao, R., Zhang, Z., An, X., Bucci, B., Perlstein, D. L., Stubbe, J., and Huang, M. (2003) *Proc. Natl. Acad. Sci. U. S. A.* **100,** 6628–6633
29. Engström, Y., Rozell, B., Hansson, H. A., Stemme, S., and Thelander, L. (1984) *EMBO J.* **3,** 863–867
30. Engström, Y., and Rozell, B. (1988) *EMBO J.* **7,** 1615–1620
31. Tanaka, H., Arakawa, H., Yamaguchi, T., Shiraishi, K., Fukuda, S., Matsui, K., Takei, Y., and Nakamura, Y. (2000) *Nature* **404,** 42–49
32. Koç, A., Wheeler, L. J., Mathews, C. K., and Merill, G. F. (2003) *J. Biol. Chem.* **278,** 9345–9352
33. Kunz, B. A., and Kohalmi, S. E. (1991) *Annu. Rev. Genet.* **25,** 339–359